J Neural Transm (2014) 121:1245–1257
DOI 10.1007/s00702-014-1185-3

NEUROLOGY AND PRECLINICAL NEUROLOGICAL STUDIES - ORIGINAL ARTICLE

6-Hydroxydopamine impairs mitochondrial function in the rat model of Parkinson's disease: respirometric, histological, and behavioral analyses

Andreas Kupsch · Werner Schmidt · Zemfira Gizatullina · Grazyna Debska-Vielhaber · Jürgen Voges · Frank Striggow · Patricia Panther · Herbert Schwegler · Hans-Jochen Heinze · Stefan Vielhaber · Frank Norbert Gellerich

Received: 16 December 2013 / Accepted: 23 February 2014 / Published online: 14 March 2014

Abstract Mitochondrial defects have been shown to be associated with the pathogenesis of Parkinson's disease (PD). Yet, experience in PD research linking mitochondrial dysfunction, e.g., deregulation of oxidative phosphorylation, with neuronal degeneration and behavioral changes is rather limited. Using the 6-hydroxydopamine (6-OHDA) rat model of PD, we have investigated the potential role of mitochondria in dopaminergic neuronal cell death in the substantia nigra pars compacta by high-resolution respirometry. Mitochondrial function was correlated with the time course of disease-related motor behavior asymmetry and dopaminergic neuronal cell loss, respectively. Unilateral 6-OHDA injections (>2.5 μg/2 μl) into the median forebrain bundle induced an impairment of oxidative phosphorylation due to a decrease in complex I activity. This was indicated by increased flux control coefficient. During the period of days 2–21, a progressive decrease in respiratory control ratio of up to −58 % was observed in the lesioned compared to the non-lesioned substantia nigra of the same animals. This decrease was associated with a marked uncoupling of oxidative phosphorylation. Mitochondrial dysfunction, motor behavior asymmetry, and dopaminergic neuronal cell loss correlated with dosage (1.25–5 μg/2 μl). We conclude that high-resolution respirometry may allow the detection of distinct mitochondrial dysfunction as a suitable surrogate marker for the preclinical assessment of potential neuroprotective strategies in the 6-OHDA model of PD.

Keywords Parkinson's disease · Respirometry · 6-OHDA model · Mitochondria complex 1 · Dopamine · Substantia nigra pars compacta · Flux control coefficients

Abbreviations

$\Delta\Psi$	Mitochondrial membrane potential
AdN	Adenine nucleotide
C_0	Flux control coefficient
Cat	Carboxyatractyloside
C_P	Pearson's correlation
E	Enzyme activity
EGTA	Ethylene glycol-bis(2-aminoethylether)-*N,N,N′,N′*-tetraacetic acid
G-3-P	Glycero-3-phosphate
G-3-PDH	G-3-P-dehydrogenase
MPTP	*N*-methyl-4-phenyl-1,2,3,6-tetrahydropyridine

A. Kupsch and W. Schmidt equally contributed as first authors.

A. Kupsch (✉) · J. Voges · P. Panther
Department of Stereotactic Neurosurgery, Otto-von-Guericke-Universität/Medizinische Fakultät, Leipziger Str. 44, 39120 Magdeburg, Germany
e-mail: andreas.kupsch@med.ovgu.de

A. Kupsch · G. Debska-Vielhaber · H.-J. Heinze · S. Vielhaber · F. N. Gellerich
Department of Neurology, Otto-von-Guericke-Universität/Medizinische Fakultät, Leipziger Str. 44, 39120 Magdeburg, Germany

W. Schmidt · F. Striggow
Laboratory of Neurodegeneration and Intervention Strategies, German Center for Neurodegenerative Diseases (DZNE), c/o ZENIT-Technologie Park, Leipziger Str. 44, 39120 Magdeburg, Germany

Z. Gizatullina · J. Voges · H.-J. Heinze · F. N. Gellerich (✉)
Department of Behavioral Neurology, Leibniz-Institute for Neurobiology, Brenneckestraße 6, 39118 Magdeburg, Germany
e-mail: frank.gellerich@ifn-magdeburg.de

H. Schwegler
Institute of Anatomy, Otto-von-Guericke-Universität/Medizinische Fakultät, Leipziger Str. 44, 39120 Magdeburg, Germany

J	Uninhibited respiration rate
MFB	Median forebrain bundle
MOPS	3-(*N*-morpholino)propanesulfonic acid
mtDNA	Mitochondrial DNA
6-OHDA	6-Hydroxydopamine
PBS	Phosphate-buffered saline
PD	Parkinson's disease
RCR	Respiratory control ratio
RCIR	Relative complex I-dependent respiratory rate
ROS	Reactive oxygen species
SN	Substantia nigra
SNPC	Substantia nigra pars compacta
TH	Tyrosine hydroxylase
TH-IR	Tyrosine hydroxylase immunoreactive

Introduction

Parkinson's disease (PD) is the second most frequent neurodegenerative disorder with a prevalence of approximately 1 % in Europe and North America (de Lau et al. 2004). It is characterized by a marked loss of dopaminergic neurons in the substantia nigra (SN) pars compacta (SNPC) leading to a reduction of dopamine in the target structure, the striatum (Fahn 2003) Dopaminergic deficits result in motor and postural disabilities, as well as cognitive and vegetative disturbances (Chaudhuri et al. 2006). The mechanisms underlying neuronal degeneration in PD are complex and are still incompletely understood, but probably reflect the end point of different environmental and genetic influences.

Several lines of evidence link the impairment of mitochondrial components such as cytochrome oxidase and mitochondrial enzymes as for instance Parkin, PINK1, DJ-1 to the pathogenesis of PD (Banerjee et al. 2009; Miller et al. 2009). Increased mutations of mitochondrial DNA and reduced activities of complex I in the SN have been associated with sporadic (Bender et al. 2006; Kraytsberg et al. 2006; Schapira 2008) and atypical PD (Baloh et al. 2007; Luoma et al. 2004). In animal models of PD, distinct mutations in mitochondrial DNA (mtDNA) of SN are sufficient to cause Parkinsonism (Ekstrand et al. 2007). Furthermore, it has been reported that mtDNA of SN in general (Soong et al. 1992) and in PD patients displays a higher mutation rate than other brain regions (Lin et al. 2012). In addition, family studies with genetically determined forms of PD have identified genes, which are involved in mitochondrial function (Schapira et al. 1989). Some of these genes, e.g., PINK1 (Koh and Chung 2012), encode exclusively for mitochondrial proteins, demonstrating that PD and associated nigrostriatal degeneration are linked to mitochondrial dysfunction. Moreover, toxins, such as MPTP (*N*-methyl-4-phenyl-1,2,3,6-tetrahydropyridine) and rotenone, which inhibit complex I of the mitochondrial respiration chain, induce Parkinsonism in animals and humans. Stereotactic injection of 6-hydroxydopamine (6-OHDA) into the nigrostriatal tract dose dependently and permanently disrupts nigrostriatal function in rats and represents the most widely used animal model of PD (Bové and Perier 2012; Hökfelt and Ungerstedt 1973; Ungerstedt 1968). Following 6-OHDA injections into the median forebrain bundle (MFB), dopaminergic neurons in the SN begin to degenerate within 12 h and exhibit a non-apoptotic morphology. As a result, marked lesions of striatal dopaminergic terminals occur within 2–3 days. 6-OHDA destroys catecholaminergic structures by a combined effect of reactive oxygen species (ROS) and quinones (Cohen 1984). Thus, various antioxidants reduce both 6-OHDA toxicity and oxidative stress (Tobon-Velasco et al. 2013b). On the other hand, it has been reported that 6-OHDA (in contrast to its oxidized derivatives) directly and reversibly inhibits complex I and complex IV of isolated brain (Glinka and Youdim 1995) and liver (Glinka et al. 1998) mitochondria.

However, due to the large complexity of mitochondria, which comprise more than 1,000 different proteins, the detection of isolated defects does not allow the conclusion that spotty defects cause mitochondrial dysfunction and cannot exclude the contribution of other defects. Therefore, a functional investigation of freshly prepared mitochondria is mandatory to quantify oxidative phosphorylation in mitochondria. To our knowledge, mitochondrial function of the SN has neither been investigated in physiological conditions (e.g., drug-naive animals) nor in the 6-OHDA model of PD. To address this issue, we have adapted high-resolution respirometry to record the time course of mitochondrial functional parameters in SN homogenates after unilateral injection of 6-OHDA into the MFB of rats over 21 days. Concomitantly, the animal's motor behavior and the corresponding number of dopaminergic neurons in SNPC were assessed by quantification of apomorphine-induced rotational asymmetry and of tyrosine hydroxylase immunoreactive (TH-IR) cells in the SNPC, respectively.

Materials and methods

Animals

Male Sprague–Dawley rats (8 weeks old, 250–280 g (Harlan Laboratories, Eystrup, Germany) were maintained under constant environmental conditions with ambient temperature of 20 ± 2 °C and relative humidity of 50 % and were housed with a 12-h light–dark cycle. Food and

water were given ad libitum. Experiments were carried out in accordance with the European Communities Council Directive (2010/63/EU). The study was approved by the authorities of the State of Saxony-Anhalt (*Landesverwaltungsamt*) and performed according to institutional and national guidelines (German Animal Protection Act, 1998).

6-OHDA-induced lesion of the median forebrain bundle

6-OHDA was unilaterally injected into the right median forebrain bundle (MFB) to induce selective cell death of dopaminergic neurons in the SN. Throughout all surgical procedures, the body temperature of animals was kept at 37 °C via a thermostatically controlled heating blanket, coupled to a rectal temperature sensor. About 4 and 2 % halothane in nitrous oxide/oxygen (70:30) were applied via a nose cone to induce and maintain anesthesia, respectively. Animals were placed in a stereotaxic frame (David Kopf Instruments, Tujunga, CA, USA). Then, a burr hole (1 mm diameter) was drilled into the skull, and a Hamilton syringe with a 29-gauge steel cannula was stereotaxically inserted using the following coordinates for MFB (Paxinos and Watson 2007): posterior +3.2 mm, lateral +1.6 mm, ventral 8.8 mm, tooth bar at −4 mm. Unilateral MFB lesions were induced by the application of 6-OHDA at different concentrations (1.25, 2.5, 4, or 5 µg) (Sigma-Aldrich, Taufkirchen, Germany) in 0.9 % sodium chloride solution (AppliChem, Darmstadt, Germany) (2 µl), containing 0.02 % (v/w) ascorbic acid over a time period of 10 min. After 6-OHDA injection, the injection needle was kept in the above position for further 5 min before slowly removing it.

Rotation behavior analysis

The rats were sequentially tested for apomorphine-induced, contralateral rotations at different time points after unilateral 6-OHDA injection into the MFB. Apomorphine (Sigma-Aldrich, Taufkirchen, Germany) was dissolved in 0.9 % (w/v) sodium chloride solution (AppliChem, Darmstadt, Germany) and was subcutaneously administered at 0.25 mg/kg body weight. After apomorphine injection, the rats were individually set into a hemispherical plastic bowl (diameter 35 cm). Starting 10 min after apomorphine application, the numbers of full contralateral rotations were visually counted for 10 min.

Immunohistochemistry

Following the last rotation behavior analysis 2, 6, 12, and 21 days post-6-OHDA injection, respectively, rats were deeply anesthetized with sodium pentobarbital (250 mg/kg, intraperitoneally). Anesthetized animals were transcardially perfused via the ascending aorta with 50 ml isotonic saline, followed by 250 ml ice-cold 4 % (w/v) paraformaldehyde in 0.1 M PBS (pH 7.4). Brains were carefully removed, post-fixed in the same fixative overnight, and subsequently placed in 30 % (w/v) sucrose in 0.1 M PBS (pH 7.4) for cryoprotection. Frontal sections, comprising the SN, were cut with a thickness of 20 µm, using a cryostat (Microm International GmbH, Walldorf, Germany). For immunohistochemistry and quantitative analysis of dopaminergic neurons free-floating sections were permeabilized with 0.2 % (v/v) Triton X-100 in 0.1 M PBS containing 10 % normal horse serum for 30 min. After washing in 0.1 M PBS, unspecific antibody binding was blocked by 10 % normal horse serum for 30 min, followed by a further wash in 0.1 M PBS. Then, sections were incubated with the primary antibodies (rabbit anti-tyrosine hydroxylase (TH) antibody; 1:1,000, Abcam, Cambridge, UK) in 2 % normal horse serum/PBS. After overnight incubation at 4 °C, sections were rinsed with 0.1 M PBS and incubated with the complementary secondary antibody Alexa Fluor 488 goat anti-rabbit IgG (1:200, Invitrogen Life Technologies, Grand Island, NY, USA). After a final wash in 0.1 M PBS, brain sections were mounted onto glass slides in Vectashield mounting medium (Vector Laboratories, Burlingame, CA, USA) containing 4′,6-diamidino-2-phenylindole (DAPI) nuclear counter stain and cover slipped.

Cell quantification

For quantitative analysis of dopaminergic neurons in the SNPC 2, 6, 12, and 21 days post-6-OHDA injection into the MFB, TH-IR neurons were counted using an inverted fluorescence microscope (ECLIPSE TE2000-S, Nikon, Düsseldorf, Germany) with a mounted CCD camera (1300QCB, VDS Vosskühler, Osnabrück, Germany) and with objectives Plan UW 10X/0.60 and Plan Flour 20X/0.13 (Carl Zeiss, Jena, Germany). Ipsi- (lesioned) and contralateral (unlesioned) SNPC of 5–8 animals per treatment group were analyzed, using Lucia software package (version 4.2.1., Nikon, Düsseldorf, Germany) or LSM 5 Pascal software package (version 4.0, Carl Zeiss, Jena, Germany) by WS (experiment 1: 1.25, 2.5, 5 µg 6-OHDA) and by FS (experiment 2: 4 µg 6-OHDA), which accounts for the differential absolute TH-IR cell counts in experiment 1 versus 2. In general, 5 sections per animal were used to analyze the number of TH-IR neurons in the SNPC (cf. Kupsch et al. 1992).

Brain preparation for functional investigation of mitochondria

Following an interval of 12 h between testing of rotational asymmetry with apomorphine and killing, rats were

anesthetized with sodium pentobarbital (250 mg/kg, i.p.) and decapitated 2, 6, 12, or 21 days after stereotactic injection of 6-OHDA. The brains were immediately removed from the skull. For the preparation of the SN, a slice with the thickness of approximately 2.0 mm of the midbrain was dissected from the most rostral end of the brain peduncles to the most rostral pole of the pons. The peduncles were removed, and two tissue blocks containing the ipsilateral (lesioned) or the contralateral (unlesioned) SN, respectively, were prepared according to the stereotactic atlas of Paxinos and Watson (2007). Ipsi- (lesioned) and contralateral (unlesioned) SNs from 3 animals were separately taken and stored in ice-cold isolation medium containing 225 mM mannitol, 75 mM sucrose, 1 mM EGTA, 20 mM MOPS, pH 7.4. After weighing, lesioned and unlesioned SNs were separately homogenized in isolation medium (1:5 w/v) with a small plastic pestle homogenizer in a 500-µl Eppendorf tube (Trumbeckaite et al. 2012).

High-resolution respirometry and inhibitor titrations

Mitochondrial function was analyzed by means of high-resolution respirometry (Gnaiger 2001). Immediately after SN homogenization, oxygen uptake rates were recorded in respirometry incubation medium A (IM-A) containing 120 mM mannitol, 60 mM KCL, 5 mM KH_2PO_4, 5 mM $MgCl_2$, 40 mM MOPS, 0.5 mM dithiothreitol, 1 mM EGTA (pH 7.4) plus 10 mM glutamate, and 2 mM malate. Fifteen microliters of SN homogenate (obtained from 3 mg SN) was used for each respirometric run. Measurements started with the permeabilization of synaptosomal membranes by the addition of 7 µg/ml digitonin (Kunz et al. 1999; Kuznetsov et al. 2008; Trumbeckaite et al. 2012). Substrate-specific rates of state 3 respiration were obtained using a modified multiple substrate-inhibitor titration protocol (Kuznetsov et al. 2008). To avoid secondary changes of mitochondrial function by the possible action of proteases, we performed all oxygraphic measurements in parallel, using 8 chambers of 4 oxygraphs (OROBOROS oxygraph-2k, Innsbruck, Austria) (Gnaiger 2001). Each chamber was kept at 30 °C. All measurements started no later than 40 min after removal of SN samples from the animals. The weight-specific oxygen consumption was calculated as the time derivative of the oxygen concentration (DATGRAPH Analysis software, OROBOROS®). Respiration rates were related to the corresponding wet weight of individual SN samples (µg) and assessed by the ratios of different specific respiratory rates measured within one respirometric run.

We applied metabolic control analysis and determined the flux control coefficients of complexes I and IV of the respiratory chain. For this, we performed titrations of the maximal respiration rates (state 3) with specific non-competitive inhibitors of complexes I and IV of the respiratory chain, namely Amytal and azide, respectively. From these titration curves, the flux control coefficients of the individual enzyme complexes of the respiratory chain can be calculated

$$C_0 = (\delta J/J)/(\delta I/K_D),$$

where dJ/dI is the initial slope of the inhibitor titration curve, J is the uninhibited respiration rate, and K_D is the K_D value of the inhibitor [170 µM for Amytal (Wiedemann et al. 1998) and 70 µM for azide (Kuznetsov et al. 1996)].

Statistical analysis

Data were analyzed using the paired, two-sample Student's t test assuming unequal variances. Data are presented as mean ± SEM, unless otherwise noted. Linear relationships between measured variables were assessed via Pearson product moment correlation (C_P) using the Sigma Plot 11. Statistical significance was accepted at $p \leq 0.05$.

Results

Behavioral and immunohistochemical analysis

In a first experimental setting, three different doses of 6-OHDA (1.25 µg, 2.5 µg, or 5 µg/2 µl) were studied with regard to their effects on rotational asymmetry after apomorphine exposure. Time points of analysis were sequentially set at 2, 6, 9, 12, 15, 19, and 21 days after 6-OHDA injection (Fig. 1a). The application of 2.5 µg or 5 µg 6-OHDA into the MFB increased the rotational asymmetry between days 2 and 21 post-6-OHDA exposure (Fig. 1a). The lowest 6-OHDA dose used in this study (1.25 µg) modestly increased rotational asymmetry over the time period studied, reaching a plateau phase after 6 days.

Unilateral 6-OHDA injection into the MFB triggered a dose-dependent degeneration of TH-IR neurons in the ipsilateral (lesioned) SNPC 21 days post-6-OHDA (Fig. 1b). The total number of TH-IR dopaminergic perikarya in the contralateral (non-lesioned) SNPC was 110.1 ± 5.6 (Fig. 1b, left bar). In contrast, only 53.7 ± 4.5 dopaminergic neurons survived the insult in the ipsilateral SNPC at a dose of 1.25 µg 6-OHDA (Fig. 1b). About 2.5 µg or 5 µg 6-OHDA ensued a more pronounced degeneration (22.5 ± 3.4 and 12.7 ± 2.9 dopaminergic neurons in SNPC, respectively, cf. Fig. 1b). The reduction in the number of TH-IR neurons in SNPC ipsilateral to the MFB lesion correlated with the increase in the rotational asymmetry of these animals at day 21 post-6-OHDA exposure.

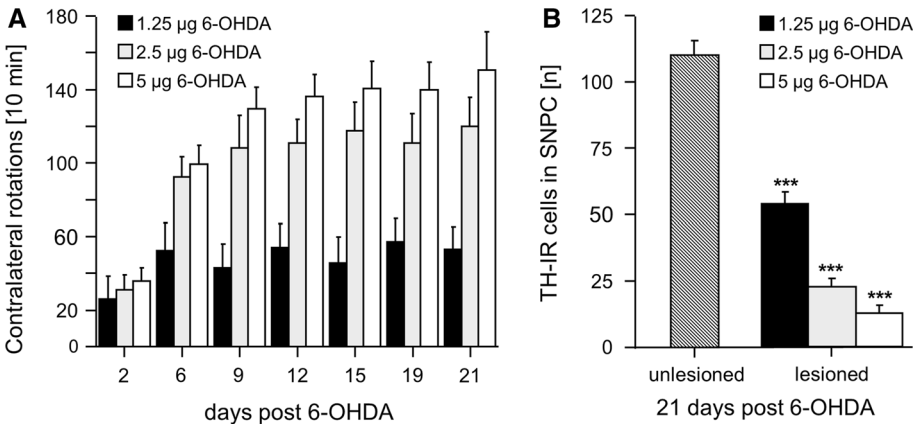

Fig. 1 Effects of 6-OHDA on motor behavior asymmetry and the number of dopaminergic neurons in the SNPC. **a** Mean number of apomorphine-induced rotations in animals 2, 6, 9, 12, 15, 19, and 21 days post-unilateral injection of different 6-OHDA doses (*black* 1.25 µg, *gray* 2.5 µg, *white* 5 µg) into the MFB ($n = 8$ rats per experimental group). **b** Quantitative analysis of the number of TH-IR cell bodies in the SNPC 21 days post-unilateral 6-OHDA exposure (*black* 1.25 µg, *gray* 2.5 µg, *white* 5 µg) into the MFB. 5–8 animals per group (1.25 µg $n = 5$, 2.5 µg $n = 8$, 5 µg $n = 8$) were killed at day 21 post-6-OHDA injection to visualize and quantify the total number of dopaminergic TH-IR neurons per section of ipsi- (lesioned) or contralateral (non-lesioned) SNPC (8 sections per rat). $***p \leq 0.001$

In the next series of experiments, we adjusted the 6-OHDA dose to 4 µg/2 µl to achieve a submaximal mitochondrial lesion and assessed the rotational asymmetry at 2, 6, and/or 12 days after 6-OHDA injection. Consistently (cf. Fig. 1), the number of apomorphine-induced, contralateral rotations increased over time (2 days: 38.4 ± 8.9, 6 days: 85.2 ± 11.4, 12 days: 112.2 ± 16.0, Fig. 2a), whereas the number of surviving, dopaminergic neurons decreased in a time-dependent manner (Fig. 2b, c). Both parameters, i.e., the number of degenerated TH-IR cells in the lesioned (ipsilateral) SNPC and the rotational asymmetry significantly correlated, complying with previous reports (Bové and Perier 2012; Ungerstedt and Arbuthnott 1970).

Detection of mitochondrial dysfunction

Mitochondrial function in lesioned (ipsilateral) and non-lesioned (contralateral) SN homogenates was studied by high-resolution respirometry as described previously (Kunz et al. 1999; Kuznetsov et al. 2008; Trumbeckaite et al. 2012). In particular, we used an advanced multi-substrate-inhibitor protocol (Gellerich et al. 2002; Kuznetsov et al. 2008; Trumbeckaite et al. 2012), which explicitly analyses the oxidation rates of the most important complex I-dependent substrates of brain mitochondria (i.e., glutamate, malate, and pyruvate) (Gellerich et al. 2012, 2013). A representative example for the demonstration of 6-OHDA-induced changes of mitochondrial function 6 days post-injection is shown in Fig. 3 comparing contralateral (non-lesioned) (Fig. 3a) and ipsilateral (lesioned) (Fig. 3b) SN from the same group of animals. SN homogenates (15 µl) were added to the incubation medium containing 10 mM glutamate and 2 mM malate. At first, we added 7 µg/ml digitonin to permeabilize synaptic and other membranes that enclose mitochondria. This procedure removes the latency of otherwise intracellular mitochondria and increases the respiration rates in general by 50 % (not shown). After addition of 2 mM ADP, the fully activated glutamate/malate-dependent respiration was measured (state $3_{glu/mal}$) (Fig. 3a). To evaluate the maximum complex I-dependent respiration, 10 mM pyruvate was subsequently added, causing a small, but significant increase in respiration (state $3_{glu/mal/pyr}$). In order to shut off the complex I-dependent respiration, the specific complex I inhibitor rotenone was added, decreasing the rate of respiration nearly to zero. Glycero-3-phosphate (G-3-P) re-activated mitochondrial respiration, since the mitochondrial G-3-P-dehydrogenase (G-3-PDH) fuels the respiratory chain with electrons independent of complex I (Gellerich et al. 2012). The rather small extent of G-3-P-dependent respiration (state $3_{G\text{-}3\text{-}P}$) indicated a low capacity of the G-3-PDH. In contrast, the following addition of succinate (state $3_{G\text{-}3\text{-}P/suc}$) provided a distinctly more pronounced effect and allowed a respiration rate as usually observed in brain mitochondria (Kunz et al. 1999; Trumbeckaite et al. 2012). Finally, carboxyatractyloside (Cat), an inhibitor of the adenine nucleotide translocator, was added to decrease the rate of respiration to the level of non-phosphorylating respiration (state $4_{G\text{-}3\text{-}P/Suc/Cat}$) (Fig. 3). According to this protocol, the respirogram of mitochondria prepared from the contralateral (unlesioned) SN revealed normal functional properties (Fig. 3a).

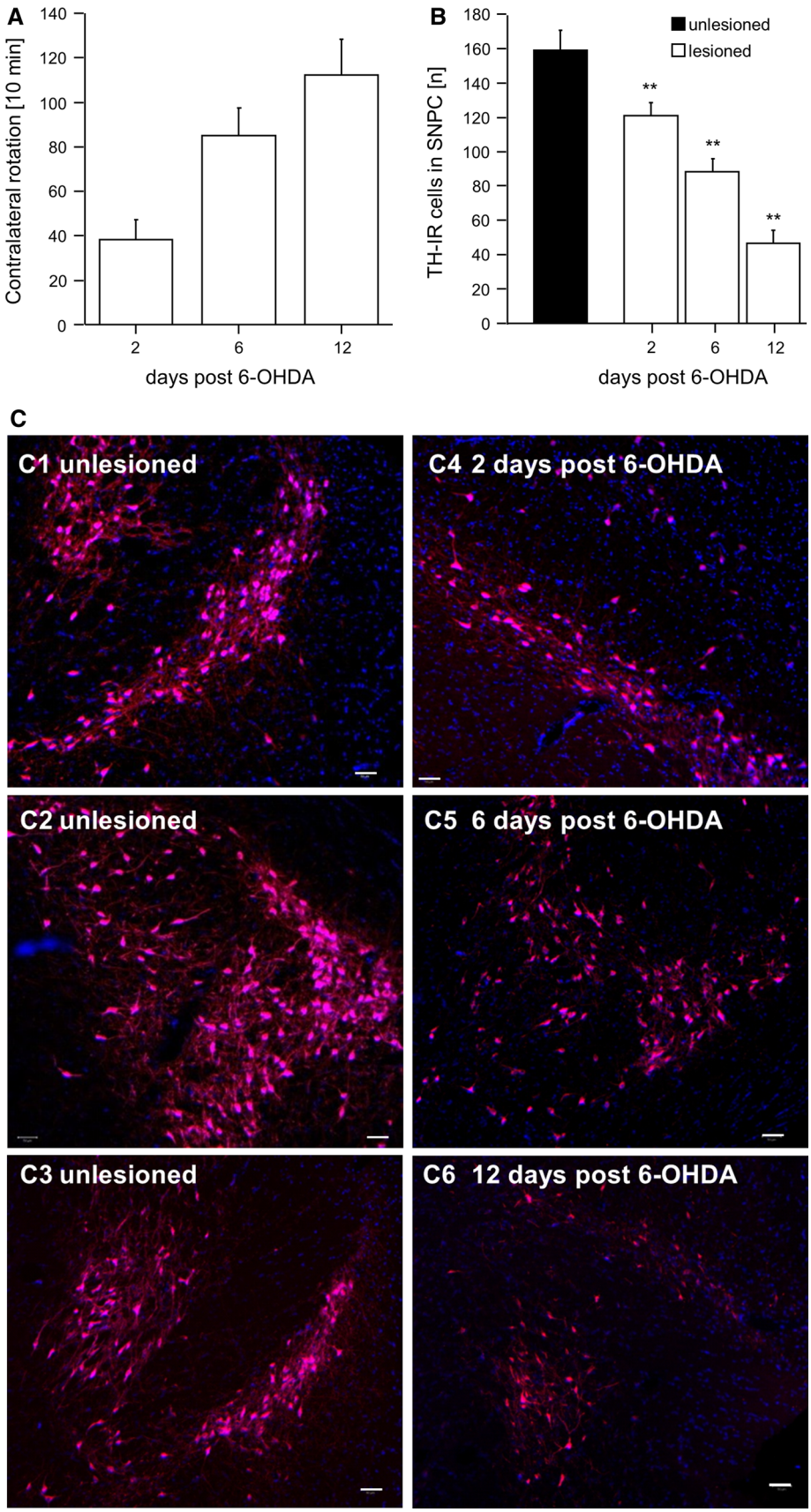

Fig. 2 Time-dependent effects of 6-OHDA on rotation behavior and on the number of TH-IR-positive neurons in the SNPC. **a** Number of apomorphine-induced contralateral rotations in rats 2, 6, 12 days after unilateral 6-OHDA (4 µg) lesion of the MFB. Data are expressed as mean number of contralateral rotations per 10 min, $n = 8$ rats per group. **b** Quantitative analysis of the mean number of TH-IR cell bodies in SNPC 2, 6, and 12 days post-unilateral injection of 6-OHDA (4 µg) into the MFB ($n = 5$ rats). **c** Representative examples of immunohistochemical localization of TH-IR dopaminergic neurons (*red* fluorescence) in the contralateral (1, 2, 3) or ipsilateral SNPC after (4, 2 days; 5, 6 days; 5, 12 days) unilateral 6-OHDA (4 µg) injection. *Scale bars* 20 µm. $^{**}p \leq 0.01$ between ipsi- (lesioned) and contralateral (unlesioned) SNPC

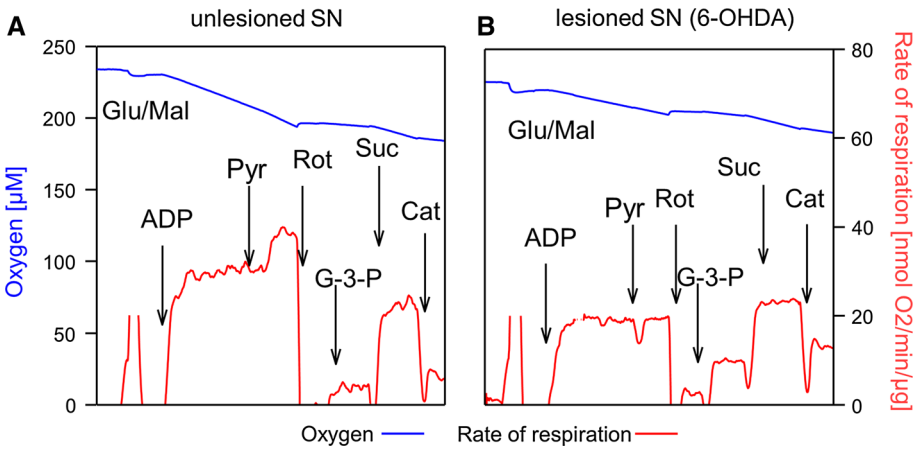

Fig. 3 Mitochondrial dysfunction in the SN after unilateral 6-OHDA injection into the MFB. Mitochondrial function was investigated using high-resolution respirometry. Homogenates (15 µl) of the lesioned and unlesioned side of SN, respectively, were added to incubation medium A. Additions: ADP, 2 mM ADP; Pyr, 10 mM pyruvate; Rot, 1.5 µM rotenone; G-3-P, 10 mM G-3-P; Suc, 10 mM succinate; Cat, 5 µM carboxyatractyloside. *Blue lines* oxygen concentration within the measuring chamber of the oxygraph. The first derivative of this signal after the time represents the rate of respiration (*red line*) in nmol O_2/min/µg tissue. Representative respirograms were selected from experiments performed 6 days after stereotactic injection of 4 µg 6-OHDA into the MFB

In contrast, mitochondria in the ipsilateral SN (exposed to 6-OHDA) were characterized by the following changes:

1. The rate of state $3_{glu/mal}$ respiration was lower than the corresponding rate of not exposed mitochondria. Moreover, pyruvate addition did not cause a further stimulation of state $3_{glu/mal}$ respiration (state $3_{glu/mal}$ = state $3_{glu/mal/pyr}$) (Fig. 3b).
2. State $3_{Glu/Mal/Pyr}$ of ipsilateral SN mitochondria was lower than their corresponding state $3_{G\text{-}3\text{-}P/Suc}$ respiration (Fig. 3b), whereas the opposite effect was observed in the non-lesioned (contralateral) SN (Fig. 3a).
3. The state $3_{G\text{-}3\text{-}P}$ of ipsilateral SN mitochondria was enlarged compared to the non-affected (contralateral) SN (Fig. 3a, b).
4. Notably, the rate of non-phosphorylating respiration (state $4_{G\text{-}3\text{-}P/Suc/Cat}$) was also increased after 6-OHDA exposure (Fig. 3a, b).

For a quantitative description of 6-OHDA-dependent changes of mitochondrial function in the ipsilateral SN as detectable in the representative experiment shown in Fig. 3, we used (1) the respiratory control ratio (RCR: state $3_{Glu/Mal/Pyr}$/state $4_{G\text{-}3\text{-}/Suc/Cat}$) and (2) the relative complex I-dependent respiration (RCIR: state $3_{Glu/Mal/Pyr}$/state $3_{G\text{-}3\text{-}P/Suc}$).

6-OHDA (2.5 µg and 5 µg) caused a significant and dose-dependent decrease in the respiratory control ratios (RCR: state $3_{Glu/Mal/Pyr}$/state $4_{G\text{-}3\text{-}/Suc/Cat}$) by 14 and 35 %, respectively (Fig. 4). Similar changes were observed for the relative complex I-dependent respiration (RCIR: state $3_{Glu/Mal/Pyr}$/state $3_{G\text{-}3\text{-}P/Suc}$) (data not shown). These data indicate that 6-OHDA doses higher than 2.5 µg, possibly

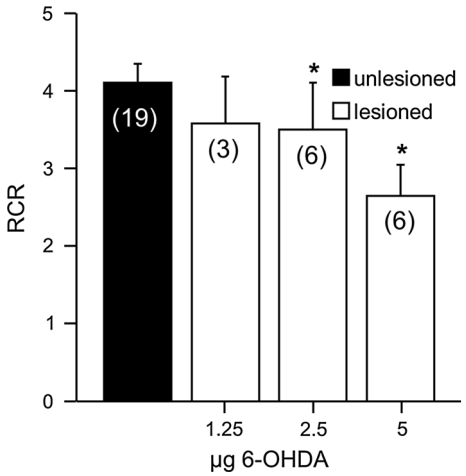

Fig. 4 6-OHDA causes mitochondrial dysfunction in the SN in a dose-dependent manner. Mitochondrial function in SN homogenates was investigated 21 days post-unilateral injection of different doses of 6-OHDA. Homogenates from lesioned (ipsilateral) or contralateral (non-lesioned) SN were analyzed. From respirograms as exemplified in Fig. 3, RCR values as the maximum complex I-dependent respiration (state $3_{Glu/Mal/Pyr}$) and succinate-dependent, non-phosphorylating respiration (state $4_{Suc/Cat}$) were calculated and plotted versus the corresponding dose of 6-OHDA. *Numbers* within the columns indicate the number of oxygraphic measurements per experimental condition. *$p < 0.05$ between ipsi- and contralateral SN

also 1.25 µg (cf. Fig. 4, low n-number in 1.25 µg 6-OHDA group), induce an impairment of mitochondrial function in the ipsilateral SN 3 weeks after 6-OHDA injection into the MFB due to diminished complex I-dependent and increased non-phosphorylating respiration rates.

Subsequently, we investigated the time course of mitochondrial changes after application of 4 µg 6-OHDA. As shown in Fig. 5a, the RCR in lesioned SN was significantly

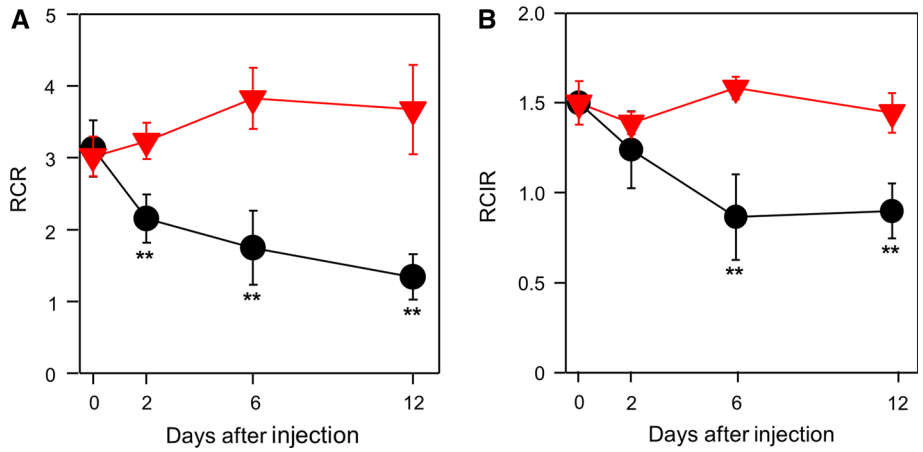

Fig. 5 Time dependency of mitochondrial dysfunction post-6-OHDA exposure. Mitochondrial function was analyzed in homogenates of lesioned SN (*black circles*) and unlesioned SN (*red triangles*). Time points after 6-OHDA injection (4 µg) as shown in Fig. 3. Two different ratios were calculated: **a** RCR values were calculated for the lesioned and unlesioned SN, respectively. **b** Relative complex I-dependent respiration (RCIR) was determined as the ratio of the maximum complex I-dependent respiration and the maximum succinate (+G-3-P)-dependent respiration. Both ratios were plotted versus the time points after 6-OHDA application in days. $^{**}p < 0.02$ between ipsi- and contralateral SN

decreased (−31 %) as early as 2 days after unilateral 6-OHDA injection, if compared to the unlesioned SN. As also illustrated in Fig. 4, these changes were caused by both a decrease in state $3_{glu/mal/pyr}$ and an increase in state $4_{G\text{-}3\text{-}/Suc/Cat}$. With increasing time after 6-OHDA treatment, this difference increased further (6 days: −45 %; 12 days: −58 %). In contrast, the RCIR in lesioned SN (Fig. 5b) was significantly decreased only 6 and 12 days after 6-OHDA injection (−43 and −41 %, respectively).

The impaired stimulation of state $3_{Glu/Mal}$ in mitochondria of lesioned SN after pyruvate addition was quantified by the ratio state $3_{Glu/Mla/Pyr}$/state $3_{Glu/Mal}$, which was significantly decreased by 16 % from 1.24 ± 0.07 in non-lesioned, compared to 1.04 ± 0.03 in lesioned SN mitochondria (Fig. 6a). The 6-OHDA-induced decrease in the latter parameter as well as the declines of RCIR and RCR described above indicate a reduction in complex I-dependent respiration. To further elucidate this assumption, a flux control analysis was performed by titrating the state 3 respiration of SN mitochondria with amytal, an inhibitor of complex I, and azide, an inhibitor of complex IV of the mitochondrial respiratory chain. The resulting flux control coefficient (Fig. 6b) C_0 for complex I of 0.29 ± 0.02 in control mitochondria of non-lesioned SN increased significantly by 48 % to 0.43 ± 0.04, whereas C_0 for complex IV was not affected in lesioned mitochondria. These data underline that 6-OHDA toxicity primarily involves a complex I-specific impairment of mitochondrial function.

The 6-OHDA-induced increase in state $3_{G\text{-}3\text{-}P}$ (Fig. 3a, b) was evaluated by the normalization of G-3-P-dependent state 3 on the state $3_{G\text{-}3\text{-}P/Suc}$ respiration (Figs. 3a, b, 6c). These ratios significantly increased in mitochondria of lesioned SN already after the second day post 6-OHDA injection and remained elevated until the day 12 (Fig. 6c).

In order to evaluate whether a compromised mitochondrial function is linked with altered histochemical and behavioral parameters in the 6-OHDA model of PD, we plotted the above RCR and RCIR data versus the number of TH-IR neurons 2, 6, and 12 days post-6-OHDA injection (Fig. 7). Based on this, we calculated the corresponding Pearson's correlation coefficients (C_P). As shown in Fig. 7, the RCR was positively correlated with the number of TH-IR cells ($C_P = 0.972$; $p = 0.0276$) in SNPC. Only a nonsignificant positive trend was observed between RCIR and the number of TH-IR cells in the SNPC ($C_P = 0.919$; $p = 0.08$). Furthermore, both RCR ($C_P = -0.974$; $p = 0.0255$) and the relative complex I-dependent respiration (RCIR) ($C_P = -0.964$; $p = -0.0361$) were negatively correlated with rotational asymmetry.

Discussion

For the first time, this study demonstrates a dose- and time-dependent impairment of oxidative phosphorylation in the ipsilateral SN of rats after unilateral 6-OHDA injection into the MFB. Mitochondrial dysfunction significantly correlated with (1) apomorphine-dependent rotation asymmetry and (2) the degeneration of TH-IR dopaminergic neurons in SNPC. The present results unravel a time- and dose-dependent mitochondrial dysfunction in the ipsilateral SN after unilateral 6-OHDA treatment. In particular, we were able to identify the crucial involvement of mitochondrial

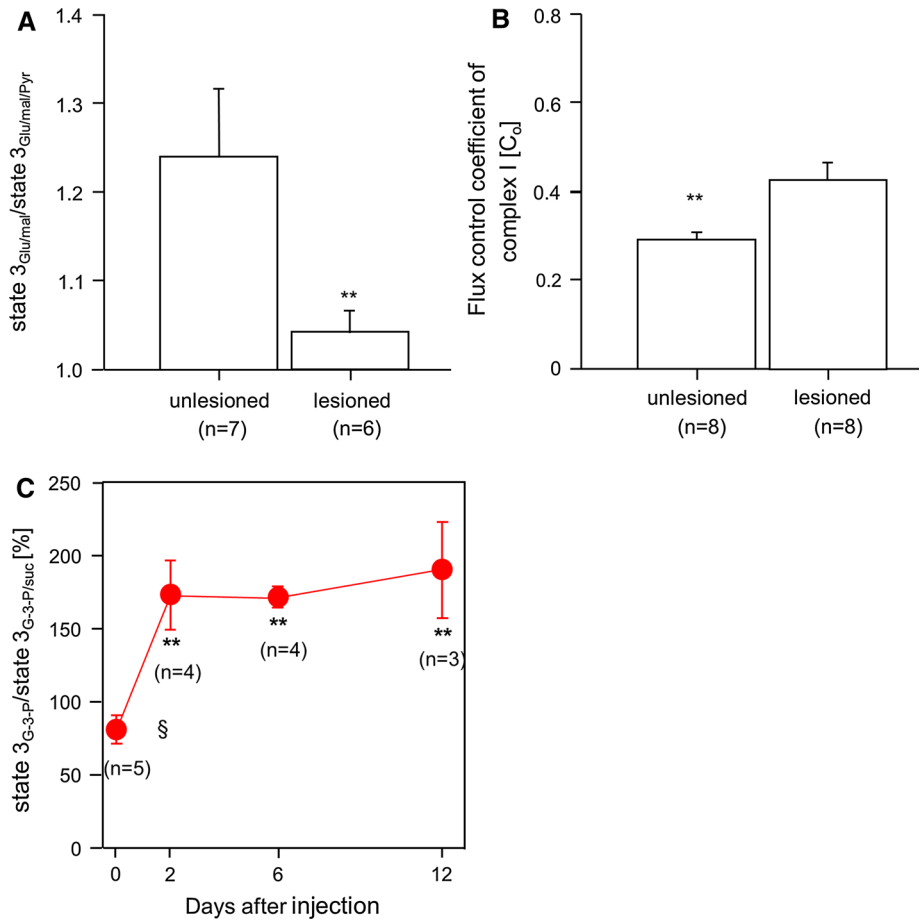

Fig. 6 6-OHDA-induced changes of mitochondrial complex I in the ipsilateral (lesioned) SN. **a** Decreased pyruvate stimulation of state $3_{Glu/Mal}$ in lesioned SN. Ratios of state $3_{Glu/Mal/Pyr}$/state $3_{Glu/Mal}$ were calculated from data measured with protocols as illustrated in Fig. 3. **b** Increased flux control coefficients of complex I in lesioned SN. Flux control coefficients were calculated from inhibitor titrations of state $3_{Glu/Mla/Pyr}$ with amytal at different time points after application of 6-OHDA. **c** Increase in G-3-P-dependent respiration in lesioned SN. Ratios of state 3_{G-3-P}/state $3_{G-3-P/Suc}$ were calculated from data measured with protocols as shown in Fig. 3 in homogenates of unlesioned and lesioned SNs at different time points after 6-OHDA injection. Data obtained for lesioned SN homogenates were related to unlesioned SN homogenates and are presented as % of corresponding values of unlesioned SN homogenates. Mitochondrial function was compared in lesioned and unlesioned SN homogenates of the same animals after injection of 4 µg 6-OHDA. *n* number of measurements. $^{**}p < 0.01$. [§]Measurement without injection

complex I and the uncoupling of oxidative phosphorylation in 6-OHDA-induced nigral neuronal cell death.

Assessment of mitochondrial function

It is generally agreed that the measurements of mitochondrial flux rates provide more reliable information about the ability of the corresponding mitochondria to generate ATP, than measurements of metabolites, membrane potentials, enzyme activities, or mutation loads, although all latter methods may add important information too (Brand and Nicholls 2011; Seppet et al. 2007). As discussed recently (Kuznetsov et al. 2008), in the present study, we used distinct tissue (SN) homogenates for assessing mitochondrial dysfunction (Kunz et al. 1999; Kuznetsov et al. 2008; Trumbeckaite et al. 2012). This well-established protocol includes a selective permeabilization of synaptosomal membranes with digitonin at low concentrations that do not affect mitochondrial membranes (Kunz et al. 1999; Kuznetsov et al. 2008; Trumbeckaite et al. 2012). The use of homogenates precludes a biased selection of a particular mitochondrial population such as synaptosomal, non-synaptosomal, normal, and pathologically altered mitochondria. Moreover, the use of homogenates allows the investigation of mitochondrial function in smaller samples.

Furthermore, it should be noted that apomorphine itself exhibits dose-dependent, anti- and pro-oxidant properties, affecting mitochondrial function in vitro (dos Santos El-Bachá et al. 2001; Gassen et al. 1996; Khaliulin et al. 2004). Clinically, there is no evidence for neurotoxicity of apomorphine (Gassen et al. 1996; Kyriazis 2003). The present design investigated ex vivo mitochondrial function

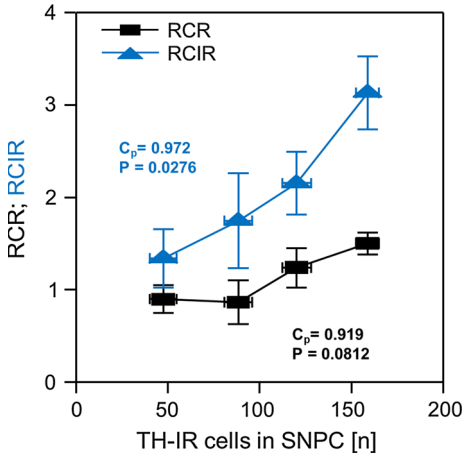

Fig. 7 Correlation between nigral mitochondrial impairment and the number of TH-IR neurons. RCR and RCIR values were determined 2, 6, and 12 day after 6-OHDA injection (taken from Fig. 5a, b) and were plotted versus TH-IR neurons assessed at the same time points. *Numbers* indicate the Pearson's correlation coefficient (C_P) and the respective p values

at least 12 h following apomorphine exposure in animals without evidence for clinical apomorphine-induced behavioral abnormalities at this time point, complying with the short half-time of apomorphine [approximately 30 min; for review cf. (Kyriazis 2003)]. Thus, it is unlikely that preceding apomorphine treatments affected the mitochondrial assessment of the present study. Independently, in the present experimental design, the contralateral non-treated SN side served as control tissue, which precludes the interpretation of the present data as being only apomorphine-related.

In particular, mitochondrial function was measured by high-resolution respirometry (Gnaiger 2001), using a refined version of a multi-substrate-inhibitor protocol (Gellerich et al. 2002; Kuznetsov et al. 2008). This procedures allowed us to examine the oxidation rates of complex I-related substrates in comparison with complex II- (succinate) and complex III-supplying (G-3-P) reactions under maximum (state 3) and non-phosphorylating conditions. Moreover, in order to selectively detect functional deficits of SN mitochondria caused by disease-related impairments of complex I of the respiratory chain and/or a defective catabolism of complex I-specific substrates (pyruvate, glutamate, malate), we evaluated two complex I-dependent states, state $3_{Glu/Mal}$ as well as state $3_{Glu/Mal/Pyr}$. In contrast to the use of isolated mitochondria, the mitochondrial content in homogenates is in principle unknown. Therefore, mitochondrial function and dysfunction is accurately described by the ratios of characteristic respiratory rates, which do not depend on the amount of mitochondria, but rather reflect mitochondrial function (Gellerich et al. 2002; Kuznetsov et al. 2008; Trumbeckaite et al. 2012). By means of flux control analysis of Heinrich and Rapoport (1974) and Kacser and Burns (1973), we further investigated the consequences of an impaired step for the whole mitochondrial metabolic system via inhibitor titrations. Consequently, we were able to calculate specific flux control coefficients, which in turn describe the contribution of the titrated enzyme in the control of the whole metabolic system (Gellerich et al. 1990).

The flux control coefficient C_0 relates changes in the overall flux through the pathway to changes in the activity of an enzyme. It is defined as the fractional change in flux divided by the fractional change in the amount of the enzyme as the change tends to zero: $C_0 = \delta J/\delta E * E/J$ with E representing enzyme activity (Heinrich and Rapoport 1974; Kacser and Burns 1973). Since C_0 of an enzyme depends on its actual activity in relation to the flux through the whole metabolic system, a decreased enzyme activity must cause an increased C_0. Therefore, the detection of an increased C_0 is an important indicator, confirming that the decreased enzyme activity limits the flux through the total system.

Mitochondrial dysfunction in the SN of 6-OHDA-treated rats

The present study allows the detection of mitochondrial impairment by direct comparison between properties of mitochondria isolated from normal and affected parts of SN in the same rats after 6-OHDA treatment. We demonstrate that the RCR, the main parameter of mitochondrial function, is distinctly impaired in the 6-OHDA model of PD, which correlated with rising 6-OHDA concentrations (Fig. 4). Significantly, decreased (−30 %) RCR values were already detected in mitochondria of lesioned SN 2 days after 6-OHDA injection into the MFB. Interestingly, a mitochondrial impairment in the striatum has been recently reported only 2–4 h after intrastriatal 6-OHDA injection as analyzed via succinate-dependent respiration (Tobon-Velasco et al. 2013a). Thus, 6-OHDA-induced mitochondrial dysfunction in the SN may also be present at earlier time points. Within the observation period of 12 days post-6-OHDA exposure, the RCR was decreased progressively (Fig. 5). The changes in RCR after 6-OHDA-induced lesion of the MFB correlated positively with the number of TH-IR cells in SNPC and negatively with the number of apomorphine-induced contralateral rotations of diseased animals (Fig. 6a).

In contrast, the reduction in RCIR reached statistical significance at later time points, i.e., 6 and 12 days after 6-OHDA injection into the MFB, indicating that the decrease in complex I-dependent respiration is delayed in comparison with the RCR changes. Notably, the significantly diminished ratio (state $3_{Glu/Mal/Pyr}$/state $3_{Glu/Mal}$) in

lesioned mitochondria complies with the finding of reduced complex I-dependent respiration. This finding could have at least two reasons:

Either (1) mitochondrial complex I itself or (2) the catabolism of complex I-dependent substrates could be impaired via 6-OHDA. By means of flux control analysis (Heinrich and Rapoport 1974; Kacser and Burns 1973), we have shown that the C_0 of complex I is significantly increased in lesioned mitochondria, whereas C_0 of complex IV remained unaffected. The increased flux control of complex I in lesioned SN mitochondria indicates the selective involvement of complex I in the neurotoxicity of 6-OHDA.

Obviously, the 6-OHDA-induced increase in state $4_{G3P,Suc,Cat}$ (Fig. 3a, b) diminishes the RCR, suggesting an uncoupling of oxidative phosphorylation without any effect on the RCIR. Thus, mitochondrial uncoupling seems also to be an important additional factor in 6-OHDA-induced mitochondrial dysfunction in the SN. Conceivably, uncoupling of oxidative phosphorylation may result from a 6-OHDA-dependent generation of ROS, leading to the opening of mitochondrial permeability transition pores (Lemasters and Nieminen 1997; Webster 2012). Interestingly, we observed significantly increased state $3_{G\text{-}3\text{-}P}$ rates in lesioned mitochondria. This unexpected result could be an indicator for a relative or compensatory increase in astrocyte numbers due to neuronal loss of DA neurons. Since astrocytes do not have a glutamate aspartate carrier (Berkich et al. 2007), their mitochondria require the mitochondrial G-3-PDH for the transport of reducing equivalents into mitochondria.

Another important issue is the potential contribution of mitochondria of dead neurons to the measured oxygen consumption under the present experimental conditions. It is generally agreed that most kinds of cell death [e.g., necrosis, apoptosis; cf. (Bredesen et al. 2006)] are initiated by impaired, dying or dead mitochondria, i.e., cells and their mitochondria die more or less at the same time. Therefore, one can assume that the contribution of "dead" mitochondria to the respirometric signal is low. If these "dead" mitochondria still respire, they may be able to consume some oxygen without changes by the metabolic state therefore increasing a little both the rates of state 4 and state 3 respiration (i.e., decreased RCIs). Decreased RCIs have been observed in numerous disease models containing morphologically intact cells (Gellerich et al. 2012). Thus, it may be assumed that the impaired mitochondrial function in our present SN homogenates mainly reflects impaired mitochondria within living cells.

It should be noted that the present experimental design did not evaluate the mechanisms of 6-OHDA-induced mitochondrial impairment. In particular, mitochondrial impairment could be a secondary phenomenon following 6-OHDA-induced nigral intoxication. Moreover, it is known that 6-OHDA causes increased ROS formation, and complex 1 is particularly sensitive for ROS-induced cell damage ["hot spot," cf. (Musatov and Robinson 2012)]. Previous in vitro studies suggest complex I inhibition in brain mitochondria following 6-OHDA exposure without the involvement of free radicals in this process (Glinka et al. 1998), although more recently it was demonstrated that 6-OHDA does not act as a primary inhibitor of the mitochondrial respiratory chain in neuroblastoma cell cultures (Giordano et al. 2012). Thus, future experiments are necessary to determine whether the distinct mitochondrial alterations observed in the present ex vivo approach precedes or follows nigral cell death.

Conclusion

The present study suggests that unilateral 6-OHDA injection into the MFB severely impairs mitochondrial function within the lesioned (ipsilateral) SN. Using high-resolution respirometry and flux control analyses, we show for the first time that mitochondrial complex I and the coupling of oxidative phosphorylation are crucially affected in the 6-OHDA model of PD. Mitochondrial dysfunction is correlated with and dopaminergic neuronal cell loss in the SNPC. Thus, distinct mitochondrial function analysis may be suitable for the preclinical identification of neuroprotective intervention strategies for PD and other neurodegenerative disorders (Olszewska and Szewczyk 2013; Vlamings et al. 2009).

Acknowledgments F.S. was supported by the Federal Ministry for Education and Research (BMBF Grant Number 03IS2211I/ProNetT3). A.K. was in part supported by Deutsche Forschungsgemeinschaft KFO 247 (Deep brain stimulation, Berlin).

We would like to thank J. Hübner and N. Huß for their excellent technical assistance.

Conflict of interest The authors reported no financial interests or potential conflicts of interest.

References

Baloh RH, Salavaggione E, Milbrandt J, Pestronk A (2007) Familial Parkinsonism and ophthalmoplegia from a mutation in the mitochondrial DNA helicase twinkle. Arch Neurol 64(7): 998–1000. doi:10.1001/archneur.64.7.998

Banerjee R, Starkov AA, Beal MF, Thomas B (2009) Mitochondrial dysfunction in the limelight of Parkinson's disease pathogenesis. Biochim Biophys Acta 1792(7):651–663. doi:10.1016/j.bbadis.2008.11.007

Bender A, Krishnan KJ, Morris CM, Taylor GA, Reeve AK, Perry RH, Jaros E, Hersheson JS, Betts J, Klopstock T, Taylor RW, Turnbull DM (2006) High levels of mitochondrial DNA deletions in substantia nigra neurons in aging and Parkinson disease. Nat Genet 38(5):515–517. doi:10.1038/ng1769

Berkich DA, Ola MS, Cole J, Sweatt AJ, Hutson SM, LaNoue KF (2007) Mitochondrial transport proteins of the brain. J Neurosci Res 85(15):3367–3377. doi:10.1002/jnr.21500

Bové J, Perier C (2012) Neurotoxin-based models of Parkinson's disease. Neuroscience 211:51–76. doi:10.1016/j.neuroscience.2011.10.057

Brand MD, Nicholls DG (2011) Assessing mitochondrial dysfunction in cells. Biochem J 435(2):297–312. doi:10.1042/BJ20110162

Bredesen DE, Rao RV, Mehlen P (2006) Cell death in the nervous system. Nature 443(7113):796–802. doi:10.1038/nature05293

Chaudhuri KR, Healy DG, Schapira AH; National Institute for Clinical E (2006) Non-motor symptoms of Parkinson's disease: diagnosis and management. Lancet Neurol 5 (3):235–245. doi:10.1016/S1474-4422(06)70373-8

Cohen G (1984) Oxy-radical toxicity in catecholamine neurons. Neurotoxicology 5(1):77–82

de Lau LM, Giesbergen PC, de Rijk MC, Hofman A, Koudstaal PJ, Breteler MM (2004) Incidence of parkinsonism and Parkinson disease in a general population: the Rotterdam Study. Neurology 63(7):1240–1244

dos Santos El-Bachá R, Daval J-L, Koziel V, Netter P, Minn A (2001) Toxic effects of apomorphine on rat cultured neurons and glial C6 cells, and protection with antioxidants. Biochem Pharmacol 61(1):73-85. doi:10.1016/S0006-2952(00)00524-4

Ekstrand MI, Terzioglu M, Galter D, Zhu S, Hofstetter C, Lindqvist E, Thams S, Bergstrand A, Hansson FS, Trifunovic A, Hoffer B, Cullheim S, Mohammed AH, Olson L, Larsson NG (2007) Progressive parkinsonism in mice with respiratory-chain-deficient dopamine neurons. Proc Natl Acad Sci USA 104(4): 1325–1330. doi:10.1073/pnas.0605208103

Fahn S (2003) Description of Parkinson's disease as a clinical syndrome. Ann N Y Acad Sci 991:1–14

Gassen M, Glinka Y, Pinchasi B, Youdim MBH (1996) Apomorphine is a highly potent free radical scavenger in rat brain mitochondrial fraction. Eur J Pharmacol 308(2):219–225. doi:10.1016/0014-2999(96)00291-9

Gellerich FN, Kunz WS, Bohnensack R (1990) Estimation of flux control coefficients from inhibitor titrations by non-linear regression. FEBS Lett 274(1–2):167–170

Gellerich FN, Deschauer M, Chen Y, Müller T, Neudecker S, Zierz S (2002) Mitochondrial respiratory rates and activities of respiratory chain complexes correlate linearly with heteroplasmy of deleted mtDNA without threshold and independently of deletion size. Biochim Biophys Acta 1556(1):41–52

Gellerich FN, Gizatullina Z, Trumbekaite S, Korzeniewski B, Gaynutdinov T, Seppet E, Vielhaber S, Heinze HJ, Striggow F (2012) Cytosolic Ca^{2+} regulates the energization of isolated brain mitochondria by formation of pyruvate through the malate-aspartate shuttle. Biochem J 443(3):747–755. doi:10.1042/BJ20110765

Gellerich FN, Gizatullina Z, Gainutdinov T, Muth K, Seppet E, Orynbayeva Z, Vielhaber S (2013) The control of brain mitochondrial energization by cytosolic calcium: the mitochondrial gas pedal. IUBMB Life 65(3):180–190. doi:10.1002/iub.1131

Giordano S, Lee J, Darley-Usmar VM, Zhang J (2012) Distinct effects of rotenone, 1-methyl-4-phenylpyridinium and 6-hydroxydopamine on cellular bioenergetics and cell death. PLoS ONE 7(9):e44610. doi:10.1371/journal.pone.0044610

Glinka YY, Youdim MB (1995) Inhibition of mitochondrial complexes I and IV by 6-hydroxydopamine. Eur J Pharmacol 292(3–4):329–332

Glinka Y, Tipton KF, Youdim MB (1998) Mechanism of inhibition of mitochondrial respiratory complex I by 6-hydroxydopamine and its prevention by desferrioxamine. Eur J Pharmacol 351(1):121–129

Gnaiger E (2001) Bioenergetics at low oxygen: dependence of respiration and phosphorylation on oxygen and adenosine diphosphate supply. Respir Physiol 128(3):277–297

Heinrich R, Rapoport TA (1974) A linear steady-state treatment of enzymatic chains. Critique of the crossover theorem and a general procedure to identify interaction sites with an effector. Eur J Biochem/FEBS 42(1):97–105

Hökfelt T, Ungerstedt U (1973) Specificity of 6-hydroxydopamine induced degeneration of central monoamine neurones: an electron and fluorescence microscopic study with special reference to intracerebral injection on the nigro-striatal dopamine system. Brain Res 60(2):269–297

Kacser H, Burns JA (1973) The control of flux. Symp Soc Exp Biol 27:65–104

Khaliulin I, Schneider A, Houminer E, Borman JB, Schwalb H (2004) Apomorphine prevents myocardial ischemia/reperfusion-induced oxidative stress in the rat heart. Free Radic Biol Med 37(7):969–976. doi:10.1016/j.freeradbiomed.2004.06.029

Koh H, Chung J (2012) PINK1 as a molecular checkpoint in the maintenance of mitochondrial function and integrity. Mol Cells 34(1):7–13. doi:10.1007/s10059-012-0100-8

Kraytsberg Y, Kudryavtseva E, McKee AC, Geula C, Kowall NW, Khrapko K (2006) Mitochondrial DNA deletions are abundant and cause functional impairment in aged human substantia nigra neurons. Nat Genet 38(5):518–520. doi:10.1038/ng1778

Kunz WS, Kuznetsov AV, Clark JF, Tracey I, Elger CE (1999) Metabolic consequences of the cytochrome c oxidase deficiency in brain of copper-deficient Mo(vbr) mice. J Neurochem 72(4):1580–1585

Kupsch A, Loschmann PA, Sauer H, Arnold G, Renner P, Pufal D, Burg M, Wachtel H, ten Bruggencate G, Oertel WH (1992) Do NMDA receptor antagonists protect against MPTP-toxicity? Biochemical and immunocytochemical analyses in black mice. Brain Res 592(1–2):74–83

Kuznetsov AV, Tiivel T, Sikk P, Kaambre T, Kay L, Daneshrad Z, Rossi A, Kadaja L, Peet N, Seppet E, Saks VA (1996) Striking differences between the kinetics of regulation of respiration by ADP in slow-twitch and fast-twitch muscles in vivo. Eur J Biochem/FEBS 241(3):909–915

Kuznetsov AV, Veksler V, Gellerich FN, Saks V, Margreiter R, Kunz WS (2008) Analysis of mitochondrial function in situ in permeabilized muscle fibers, tissues and cells. Nat Protoc 3(6):965–976. doi:10.1038/nprot.2008.61

Kyriazis M (2003) Neuroprotective, anti-apoptotic effects of apomorphine. J Anti Aging Med 6(1):21–28. doi:10.1089/1094545033765361551

Lemasters JJ, Nieminen AL (1997) Mitochondrial oxygen radical formation during reductive and oxidative stress to intact hepatocytes. Biosci Rep 17(3):281–291

Lin MT, Cantuti-Castelvetri I, Zheng K, Jackson KE, Tan YB, Arzberger T, Lees AJ, Betensky RA, Beal MF, Simon DK (2012) Somatic mitochondrial DNA mutations in early Parkinson and incidental Lewy body disease. Ann Neurol 71(6): 850–854. doi:10.1002/ana.23568

Luoma P, Melberg A, Rinne JO, Kaukonen JA, Nupponen NN, Chalmers RM, Oldfors A, Rautakorpi I, Peltonen L, Majamaa K, Somer H, Suomalainen A (2004) Parkinsonism, premature menopause, and mitochondrial DNA polymerase gamma mutations: clinical and molecular genetic study. Lancet 364(9437):875–882. doi:10.1016/S0140-6736(04)16983-3

Miller RL, James-Kracke M, Sun GY, Sun AY (2009) Oxidative and inflammatory pathways in Parkinson's disease. Neurochem Res 34(1):55–65. doi:10.1007/s11064-008-9656-2

Musatov A, Robinson NC (2012) Susceptibility of mitochondrial electron-transport complexes to oxidative damage. Focus on cytochrome c oxidase. Free Radic Res 46(11):1313–1326. doi:10.3109/10715762.2012.717273

Olszewska A, Szewczyk A (2013) Mitochondria as a pharmacological target: magnum overview. IUBMB Life 65(3):273–281. doi:10.1002/iub.1147

Paxinos G, Watson C (2007) The rat brain in stereotaxic coordinates. Academic, New York

Schapira AH (2008) Mitochondria in the aetiology and pathogenesis of Parkinson's disease. Lancet Neurol 7(1):97–109. doi:10.1016/S1474-4422(07)70327-7

Schapira AH, Cooper JM, Dexter D, Jenner P, Clark JB, Marsden CD (1989) Mitochondrial complex I deficiency in Parkinson's disease. Lancet 1(8649):1269

Seppet E, Gizatullina Z, Trumbeckaite S, Zierz S, Striggow F, Gellerich FN (2007) Mitochondrial medicine: the central role of cellular energetic depression and mitochondria in cell pathophysiology. In: Molecular System Bioenergetics. Wiley, New York, pp 479–520. doi:10.1002/9783527621095.ch15

Soong NW, Hinton DR, Cortopassi G, Arnheim N (1992) Mosaicism for a specific somatic mitochondrial DNA mutation in adult human brain. Nat Genet 2(4):318–323. doi:10.1038/ng1292-318

Tobon-Velasco JC, Limon-Pacheco JH, Orozco-Ibarra M, Macias-Silva M, Vazquez-Victorio G, Cuevas E, Ali SF, Cuadrado A, Pedraza-Chaverri J, Santamaria A (2013a) 6-OHDA-induced apoptosis and mitochondrial dysfunction are mediated by early modulation of intracellular signals and interaction of Nrf2 and NF-kappaB factors. Toxicology 304:109–119. doi:10.1016/j.tox.2012.12.011

Tobon-Velasco JC, Palafox-Sanchez V, Mendieta L, Garcia E, Santamaria A, Chamorro-Cevallos G, Limon ID (2013b) Antioxidant effect of Spirulina (Arthrospira) maxima in a neurotoxic model caused by 6-OHDA in the rat striatum. J Neural Transm. doi:10.1007/s00702-013-0976-2

Trumbeckaite S, Gizatullina Z, Arandarcikaite O, Rohnert P, Vielhaber S, Malesevic M, Fischer G, Seppet E, Striggow F, Gellerich FN (2012) Oxygen glucose deprivation causes mitochondrial dysfunction in cultivated rat hippocampal slices: protective effects of CsA, its immunosuppressive congener [D-Ser](8)CsA, the novel non-immunosuppressive cyclosporin derivative Cs9, and the NMDA receptor antagonist MK 801. Mitochondrion. doi:10.1016/j.mito.2012.07.110

Ungerstedt U (1968) 6-Hydroxy-dopamine induced degeneration of central monoamine neurons. Eur J Pharmacol 5(1):107–110

Ungerstedt U, Arbuthnott GW (1970) Quantitative recording of rotational behavior in rats after 6-hydroxy-dopamine lesions of the nigrostriatal dopamine system. Brain Res 24(3):485–493

Vlamings R, Visser-Vandewalle V, Kozan R, Kaplan S, Steinbusch HW, Temel Y (2009) Bilateral high frequency stimulation of the subthalamic nucleus normalizes COX activity in the substantia nigra of Parkinsonian rats. Brain Res 1288:143–148. doi:10.1016/j.brainres.2009.06.091

Webster KA (2012) Mitochondrial membrane permeabilization and cell death during myocardial infarction: roles of calcium and reactive oxygen species. Futur Cardiol 8(6):863–884. doi:10.2217/fca.12.58

Wiedemann FR, Winkler K, Kuznetsov AV, Bartels C, Vielhaber S, Feistner H, Kunz WS (1998) Impairment of mitochondrial function in skeletal muscle of patients with amyotrophic lateral sclerosis. J Neurol Sci 156(1):65–72